# Inhibition of STAT3 reverses alkylator resistance through modulation of the AKT and β-catenin signaling pathways

YONGZHI WANG[1], LINGCHAO CHEN[2], ZHAOSHI BAO[1], SHOUWEI LI[3], GAN YOU[1], WEI YAN[1], ZHENDONG SHI[4], YANWEI LIU[1], PEI YANG[1], WEI ZHANG[1], LEI HAN[4], CHUNSHENG KANG[4-6] and TAO JIANG[1]

[1]Glioma Center, Department of Neurosurgery, Beijing Tiantan Hospital, Capital Medical University, Beijing 100050; [2]Department of Neurosurgery, The Second Affiliated Hospital, Harbin Medical University, Harbin 150086; [3]Department of Neurosurgery, Beijing Sanbo Brain Hospital, Capital Medical University, Beijing 100093; [4]Department of Neurosurgery, Laboratory of Neuro-Oncology, Tianjin Medical University General Hospital, Tianjin 300052; [5]Key Laboratory of Post-Trauma Neuro-Repair and Regeneration in the Central Nervous System, Ministry of Education, Tianjin 300052; [6]Tianjin Key Laboratory of Injuries, Variations and Regeneration of the Nervous System, Tianjin 300052, P.R. China

Received June 1, 2011; Accepted July 4, 2011

DOI: 10.3892/or.2011.1396

**Abstract.** Activation of signal transducer and activator of transcription 3 (STAT3) is associated with poor clinical outcome of glioblastoma (GBM). However, the role of STAT3 in resistance to alkylator-based chemotherapy remains unknown. Here, we retrospectively analyzed the phosphorylated STAT3 (p-STAT3) profile of 68 GBM patients receiving alkylator therapy, identifying p-STAT3 as an independent unfavorable prognostic factor for progression-free and overall survival. Additionally, elevated p-STAT3 expression correlated with resistance to alkylator therapy. *In vitro* analysis revealed that U251 and U87 human glioma cells were refractory to treatment with the common alkylating agent temozolomide (TMZ), with only a modest impact on AKT and β-catenin activation in the context of high p-STAT3. Inhibition of STAT3 in these cells significantly enhanced the effect of TMZ. Inhibition of STAT3 dramatically decreased the $IC_{50}$ of TMZ, increasing TMZ-induced apoptosis while up-regulating expression of Bcl-2 and down-regulating expression of Bax. Furthermore, inhibition of STAT3 increased TMZ-induced $G_0$-$G_1$ arrest and decreased Cyclin D1 expression compared to TMZ alone. Together, these results indicate that inhibition of STAT3 sensitizes glioma cells to TMZ, at least in part, by blocking the p-AKT and β-catenin pathways. These findings strongly support the hypothesis that STAT3 inhibition significantly improves the clinical efficacy of alkylating agents.

*Correspondence to:* Dr Tao Jiang, Glioma Center, Department of Neurosurgery, Beijing Tiantan Hospital, Beijing 100050, P.R. China
E-mail: taojiang1964@yahoo.com.cn

Dr Chunsheng Kang, Department of Neurosurgery, Laboratory of Neuro-Oncology, Tianjin Medical University General Hospital, Tianjin 300052, P.R. China
E-mail: kang97061@yahoo.com

*Key words:* glioblastoma, p-STAT3, clinical outcome, chemoresistance, AKT, β-catenin

## Introduction

Glioblastoma multiforme (GBM) is the most common and aggressive primary malignant brain tumor. Despite intensive multimodality treatment, including surgical resection combined with radiation and chemotherapy, the prognosis of GBM patients remains very poor with a median survival of less than 15 months (1). Intrinsic or acquired chemoresistance to alkylating agents has been identified as a major cause of treatment failure; however, the molecular mechanism of resistance remains unknown (2). Signal transducer and activator of transcription 3 (STAT3) is an oncogenic transcription factor (3,4) that is constitutively active in many types of human cancers, including GBM (5,6). STAT3 regulates the transcription of multiple genes involved in cell cycle progression, cell survival and angiogenesis. As high levels of phosphorylated STAT3 in GBM correlate with a poor clinical outcome (5,6), targeting STAT3 represents a promising approach to chemosensitize GBM to alkylating agent therapeutics (7,8).

Dysregulation of proteins involved in apoptosis signal transduction (2) and cell cycle progression (9) have been implicated in the development of chemoresistance in malignant glioma. For example, up-regulation of anti-apoptotic Bcl-2 or positive cell cycle regulator Cyclin D1, or down-regulation of pro-apoptotic protein Bax, disrupt the normal apoptotic response to DNA damage. Accumulating evidence suggests that the p-AKT and β-catenin signaling pathways are involved in apoptosis-regulation (10-12). Activation of β-catenin has been shown to regulate transcription of Cyclin D1 (11), while activation of AKT is involved in inactivating pro-apoptotic factors Bad and caspase-9, activating IκB kinase- and NF-κB-induced transcription of anti-apoptotic genes, and promoting

nuclear entry of Mdm2 to inhibit the p53 pathway (13). To date, however, whether STAT3-induced alkylator-resistance is related to the mechanism of apoptosis-regulation though the p-AKT and β-catenin pathways remains unknown.

Here, we investigated the prognostic relevance of STAT3 phosphorylation at Y705 (pY705-STAT3) in a retrospective analysis of GBM patients exposed to alkylating agent therapy. Our results revealed that p-STAT3 overexpression was correlated with alkylator-resistance in a statistically significant manner. Based upon these findings, we demonstrated that pharmacologic inhibition of STAT3 with WP1066 (14) impacts p-AKT and β-catenin expression in human glioblastoma U251 and U87 cells. Furthermore, while TMZ displayed only a modest impact on AKT and β-catenin when p-STAT3 expression was high, the effect was greatly enhanced upon inhibition of STAT3. Similarly, TMZ-induced apoptosis, cell death and inhibition of cell cycle progression were enhanced following treatment with WP1066. These results suggest that inhibition of STAT3 sensitizes human glioblastoma cells to TMZ, at least in part, by blocking the p-AKT and β-catenin pathways.

## Materials and methods

*Patients and treatment*. We retrospectively identified patients with supratentorial GBM that had undergone surgical resection at the Glioma Treatment Center of Beijing Tiantan Hospital between February 2006 and April 2009. The inclusion criteria in this study were as follows: i) patients received standard treatment; ii) patients received routine contrast-enhanced MRI examination before and after surgical operation every 3 months until death; iii) patient tissue was available for immunochemical analysis; and iv) patients provided informed written consent. Patients who died from non-glioma-related causes were excluded from the study. Two independent neuropathologists reaffirmed the histological diagnosis of each patient according to the 2007 WHO Classification (15). Clinical data, including age at diagnosis, gender and preoperative Karnofsky performance status (KPS) were obtained from the patient medical charts. Progression-free survival (PFS) was defined as the time from surgical resection to the first MRI-confirmed recurrence or until death. Overall survival (OS) was defined as the period of time from surgical resection to death. The study was approved by the Ethics Committee of Beijing Tiantan Hospital and was based on the criteria of the Helsinki convention.

Standard treatment consisted of surgical resection and postoperative radiotherapy, with adjuvant chemotherapy. The extent of resection was assessed using postoperative enhanced MRI within 24 h and graded as total or subtotal resection. The patients received standard radiotherapy (60 Gy in 2 Gy fractions, with five fractions administered per week) of the contrast-enhancing lesion (plus a 2-cm safety margin and the area of preoperative edema). Adjuvant chemotherapy was administered for 4 weeks, and consisted mainly of temozolomide (TMZ) or 1-(4-amino-2-methylpyrimidinyl) methyl-3-(2-chloroethyl)-3-nitrosourea hydrochloride (ACNU) plus cisplatin or ACNU plus teniposide. Six cycles were administered in the absence of disease progression or irreversible hematological toxicity.

*Tissue microarray and immunochemistry*. Tumor regions on each formalin-fixed, paraffin-embedded tissue block were marked by a neuropathologist. Tissue microarray (TMA) blocks were constructed with a tissue microarrayer (Beecher Instruments, USA) as described previously (16). Each tumor was sampled in duplicate, yielding composite array blocks comprising a total of 132 tissue cores. In addition, the TMA also contained eight normal brain tissues from epilepsy surgical resections. Standard immunohistochemistry was applied. We used anti-p-STAT3 (tyrosine 705; rabbit monoclonal antibody, clone D3A7; Cell Signaling) at a dilution of 1:50. The degree of immunostaining was determined by combining the proportion of positively stained tumor cells and the intensity of staining. The proportion of positively stained tumor cells was graded as follows: 0, no positive tumor cells; 1, <5% positive tumor cells; 2, 5-20% positive tumor cells; and 3, >20% positive tumor cells (5). The intensity of staining was recorded on a scale of 0 (no staining), 1 (weak staining, light yellow), 2 (moderate staining, yellowish brown) and 3 (strong staining, brown). The staining index was calculated as follows: staining index = staining intensity x proportion of positively stained tumor cells. High p-STAT3 expression was defined as a staining index score >4, while low expression was defined as a staining index ≤4.

*Cell lines and cell culture*. Human glioblastoma cell lines U251 and U87 were obtained from the China Academia Sinica cell repository (Shanghai, China). The cells were maintained in Dulbecco's modified Eagle's medium (DMEM; Gibco, USA) supplemented with 10% fetal bovine serum and incubated at 37˚C in 5% $CO_2$. Cells were seeded in flasks and incubated at 37˚C in a fully humidified atmosphere with 5% $CO_2$. Upon 80% confluency, cells were starved in DMEM with 1% FBS for 24 h and maintained in this low serum condition for the course of treatment.

*Cell cycle analysis*. Cell cycle analysis by flow cytometry (FCM) was performed on transfected and control cells in log phase growth. Cells were washed with PBS, fixed with 90% ethanol overnight at 4˚C, and then incubated with RNase at 37˚C for 30 min. The nuclei of cells were stained with propidium iodide (PI) for an additional 30 min. The stained nuclei were then analyzed using a FACSCalibur flow cytometer (Becton-Dickinson, San Jose, CA, USA). Samples were analyzed by flow cytometry for the FL-2 area, and DNA histograms were analyzed by Modifit software.

*Cell viability assay*. Cell viability was determined by the MTT [3-(4,5-dimethylthiazole)-2,5-diphenyltetrazolium bromide] assay. Briefly, U87 and U251 cells were seeded into 96-well plates at 4000 cells per well and allowed to attach overnight. TMZ (Sigma, USA) or WP1066 (Calbiochem, Germany) was added to the culture at a concentration of 10 and 3 $\mu$M, respectively. On each day for 6 consecutive days after treatment, MTT solution (5 mg/ml) was added to each well, and the cells were incubated at 37˚C for 4 h. Cells were lysed, and the optical density (OD) was measured at the wavelength of 570 nm. $IC_{50}$ values were calculated from the linear regression line of the plot of percent inhibition versus log inhibitor concentration.

*Apoptosis assay*. To quantify drug-induced apoptosis, Annexin V/PI staining was performed and cells were evaluated by flow cytometry. Briefly, cells were treated with WP1066 or

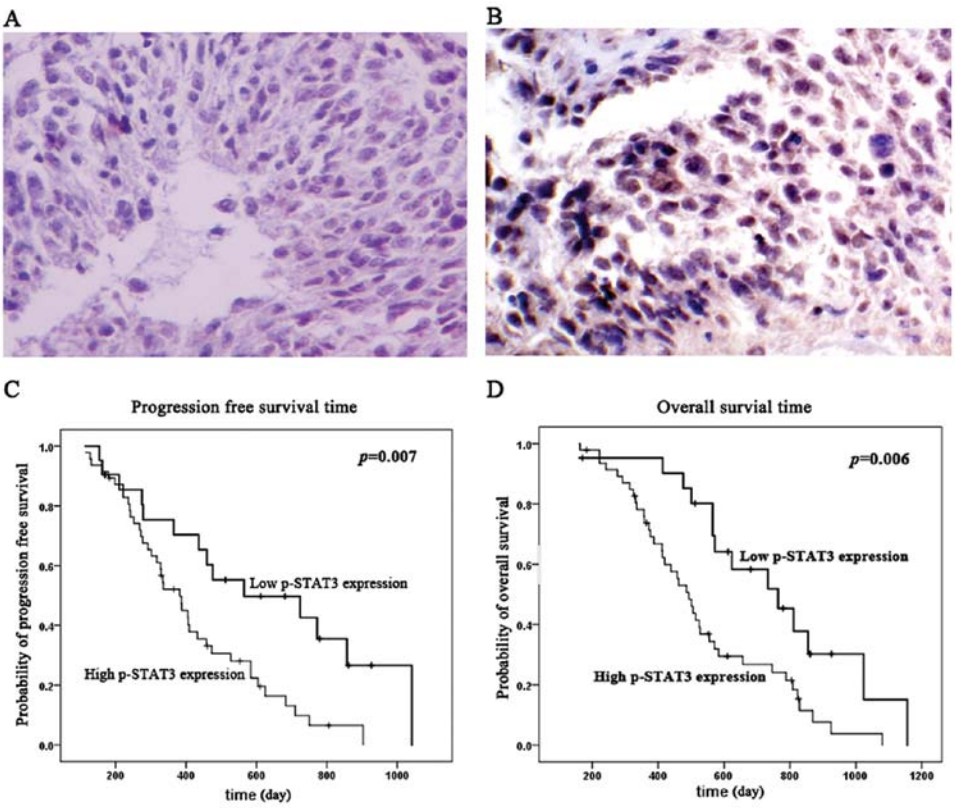


Figure 1. p-STAT3 expression correlates with progression and prognosis of GBM. Immunohistochemical staining showing a GBM specimen with low (A) and high (B) pY705-STAT3 expression (original magnification x400). Kaplan-Meier survival estimates of progression-free survival (C) and overall survival (D) according to the p-STAT3 expression level in 68 GBM patients treated with alkylating agent chemotherapy.

TMZ for 48 h, and floating and attached cells were collected. Apoptotic cells were detected using the Annexin V-FITC Apoptosis Detection Kit (BioVision, Palo Alto, CA), according to the manufacturer's instructions. The resulting fluorescence was measured by flow cytometry using a FACS flow cytometer. Tests were repeated in triplicate.

*Western blot analysis*. After cell treatment, cell lysates were prepared via sonication, electrophoresed onto SDS-polyacrylamide gels, and transferred to polyvinylidene difluoride membranes, as previously described (17). Membranes were probed with rabbit antibodies against STAT3 (79D7; Cell Signaling), pY705-STAT3 (D3A7; Cell Signaling), p-AKT (Ser473; Cell Signaling), β-catenin (H-102; Santa Cruz Biotechnology) and Cyclin D1 (c-20; Santa Cruz Biotechnology) and mouse monoclonal antibodies against Bcl-2 (C-2; Santa Cruz Biotechnology), Bax (6D149; Santa Cruz Biotechnology) and GAPDH (A-3; Santa Cruz Biotechnology) at dilutions of 1:1000. Blots were detected with horseradish peroxidase-labeled anti-rabbit or anti-mouse antibodies (1:5000 dilution), developed using enhanced chemiluminescence (ECL) reagents (Amersham Pharmacia, UK) and visualized using the Gene-Genius Imaging System (Syngene, Frederick, MD, USA).

*Statistical analysis*. SPSS 13.0 (Chicago, IL, USA) was used for all statistical analyses. Survival curves were estimated using the Kaplan-Meier method, and statistical differences were evaluated using the two-sided log-rank test. Factors with corresponding P-values of <0.05 in the univariate analysis were introduced into multivariate Cox models. The t-test, $\chi^2$ test or one-way ANOVA was applied for statistical analysis of the correlation between two independent variables. All laboratory tests were conducted in triplicate, and data were presented as the mean ± SD of separate experiments. P<0.05 (two-sided) was considered statistically significant.

## Results

*Patient demographics*. Sixty-eight mainland Han Chinese GBM patients receiving standard treatment were included in this study. The patient population consisted of 47 males and 21 females with a median age of 45 years (range 15-68). Of the 68 cases, 34 underwent total tumor resection and 34 underwent subtotal tumor resection. Preoperative KPS scores ranged from 50 to 100 (median of 80). Fifty-one patients died after a median follow-up of 29.5 months (range 15-54). The median PFS time was 406 days [95% confidence interval (CI), 347-465], and median OS time was 555 days (95% CI, 487-623).

*High p-STAT3 expression predicts poor prognosis of GBM for alkylator therapy*. Immunohistochemical detection of p-STAT3 revealed that tissue samples from 47 patients (69.1%) displayed high expression while samples from 21 patients (30.9%) displayed low expression. Eight control samples displayed low or no p-STAT3 expression. Expression of p-STAT3 was correlated with PFS and OS by univariate analysis (P=0.007 and 0.006, respectively). While patients displaying high p-STAT3 expression had median PFS and

Table I. Variables related to progression-free survival (PFS) in 68 glioblastomas with combined treatment: univariate and multivariate analysis.

| | | Univariate analysis | | | Multivariate analysis | | |
|---|---|---|---|---|---|---|---|
| Variable | No. of patients | Median PFS (days) | 95% CI (days) | P-value | Relative risk | 95% CI | P-value |
| Gender | | | | | | | |
| Male | 41 | 409 | 328-490 | | | | |
| Female | 27 | 405 | 231-579 | 0.390 | | | |
| Age (years) | | | | | | | |
| <45 | 32 | 406 | 281-531 | | | | |
| ≥45 | 36 | 432 | 352-512 | 0.729 | | | |
| KPS | | | | | | | |
| <80 | 29 | 302 | 178-426 | | | | |
| ≥80 | 39 | 360 | 426-704 | 0.010 | 0.449 | 0.258-0.782 | 0.005 |
| Extent of resection | | | | | | | |
| Subtotal | 34 | 406 | 305-507 | | | | |
| Total | 34 | 432 | 347-465 | 0.105 | | | |
| p-STAT3 expression | | | | | | | |
| Low | 21 | 565 | 130-999 | | | | |
| High | 47 | 382 | 303-460 | 0.007 | 2.629 | 1.362-5.073 | 0.004 |

Table II. Variables related to OS in 68 glioblastomas with combined treatment: univariate and multivariate analysis.

| | | Univariate analysis | | | Multivariate analysis | | |
|---|---|---|---|---|---|---|---|
| Variable | No. of patients | Median OS (days) | 95% CI (days) | P-value | Relative risk | 95% CI | P-value |
| Gender | | | | | | | |
| Male | 41 | 565 | 466-564 | | | | |
| Female | 27 | 555 | 485-565 | 0.468 | | | |
| Age (years) | | | | | | | |
| <45 | 32 | 565 | 281-531 | | | | |
| ≥45 | 36 | 527 | 421-623 | 0.652 | | | |
| KPS | | | | | | | |
| <80 | 29 | 462 | 379-545 | | | | |
| ≥80 | 39 | 733 | 487-979 | 0.002 | 0.368 | 0.205-0.663 | 0.001 |
| Extent of resection | | | | | | | |
| Subtotal | 34 | 493 | 408-548 | | | | |
| Total | 34 | 746 | 477-1015 | 0.010 | | | |
| p-STAT3 expression | | | | | | | |
| Low | 21 | 764 | 550-978 | | | | |
| High | 47 | 493 | 423-563 | 0.006 | 2.402 | 1.268-4.550 | 0.007 |

CI, confidence interval; KPS, Karnofsky performance status.

OS times of 382 and 493 days, respectively, those with low expression had PFS and OS times of 565 and 764 days, respectively. Preoperative KPS score and extent of resection was also related to OS (P=0.002 and 0.01, respectively). No statistical significance was observed between age or gender and either PFS or OS (Fig. 1, Tables I and II).

Multivariate analysis identified that high p-STAT3 expression was a significant independent unfavorable prognostic factor for PFS [P=0.004, hazard ratio (HR), 2.629] and OS (P=0.007, HR, 2.402) (Tables I and II). Similarly, preoperative KPS score was also identified as an independent prognostic factor for PFS (P=0.005) and OS (P=0.001).

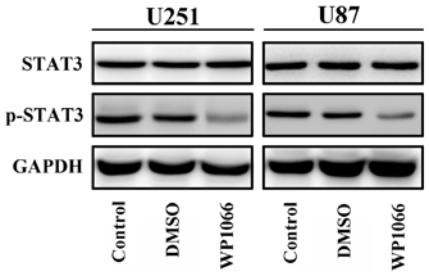


Figure 2. Effect of WP1066 on STAT3 activation in U251 and U87 cells. Western blot analysis of U251 and U87 cell extracts 48 h following treatment with 3 $\mu$M WP1066. The expression of GAPDH was examined to ensure uniform protein loading in all lanes.

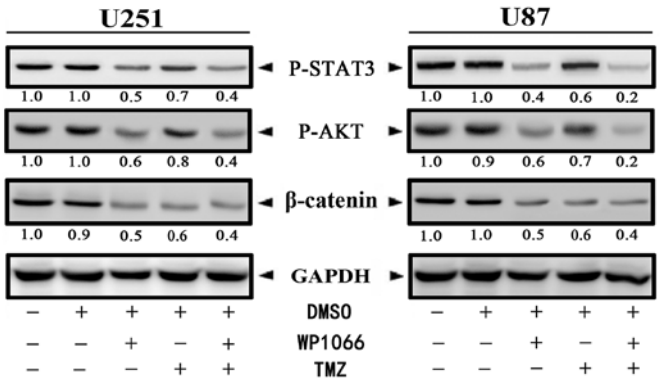


Figure 3. p-STAT3 regulates p-AKT and β-catenin activation in response to TMZ. U251 and U87 cells were cultured in the presence of TMZ (10 $\mu$M) and/or WP1066 (3 $\mu$M) for 48 h. Western blot analysis of protein extracts for p-STAT3, p-AKT and β-catenin was performed. For each sample, the densitometric levels were normalized to the respective levels of GAPDH. The results are representative of three independent experiments.

*WP1066 inhibits constitutively activated STAT3 in U251 and U87 cells*. Western blot analysis identified high expression of pY705-STAT3 in the U251 and U87 human glioblastoma cell lines (Fig. 2). A previous study showed that WP1066 was an effective inhibitor of STAT3 and its upstream regulator JAK2 (14). It was demonstrated that WP1066, at the low-cytotoxic concentration of 3 $\mu$M for 48 h (18), inhibited up to 50% of STAT3 phosphorylation at Y705 without significantly altering total STAT3 expression (Fig. 2). These data demonstrate that WP1066 inhibits constitutively activated STAT3 at Y705.

*p-STAT3 regulates TMZ-induced activation of the PI3K/AKT and Wnt/β-catenin pathways*. The phosphatidylinositol 3-kinase (PI3K)/AKT pathway in malignant cells contributes to survival signaling (12,13). Previous studies have shown that the activity of the PI3K/AKT pathway in tumors is linked to resistance to antineoplastic agents (19,20). We examined p-AKT expression following treatment with the novel alkylating agent TMZ. We observed that in the context of high p-STAT3, low-dose TMZ (10 $\mu$M) resulted in a modest inhibition of AKT activation, such that p-AKT was decreased by 20% in U251 cells and 30% in U87 cells. Inhibition of STAT3 by WP1066 significantly enhanced TMZ-induced AKT inhibition. In cells treated with WP1066 (resulting in a 60% reduction in p-STAT3), TMZ-induced AKT inhibition was decreased by 60 and 80% in U251 and U87 cells, respectively. In summary, a 40% reduction in activated STAT3 enhanced TMZ-induced inhibition of p-AKT by ~2- and 3.5-fold in U251 and U87 cells, respectively (Fig. 3).

Aberrant activation of the β-catenin signaling pathway is similarly associated with cancers, as multiple Wnt/β-catenin target genes are regulators of cell proliferation, survival and

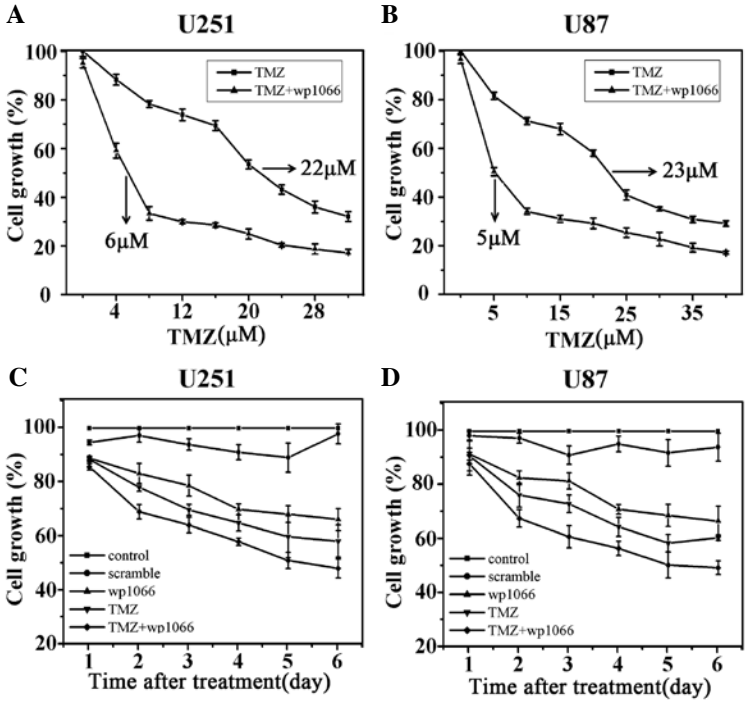


Figure 4. TMZ-induced inhibition of STAT3 impacts U251 and U87 cell viability. Viability of U251 (A) and U87 (B) cells 48 h following treatment with WP1066, TMZ or the indicated combinations, as determined by the MTT assay. Absorbance at 570 nm was normalized to controls (untreated cells) to determine cell viability. An aqueous solution of TMZ and WP1066 was added to U251 (C) and U87 (D) cells and incubation was carried out for 6 days. A drug-induced decrease in cell numbers was determined using the MTT assay. Values represent the mean ± SD (n=3 replicates).

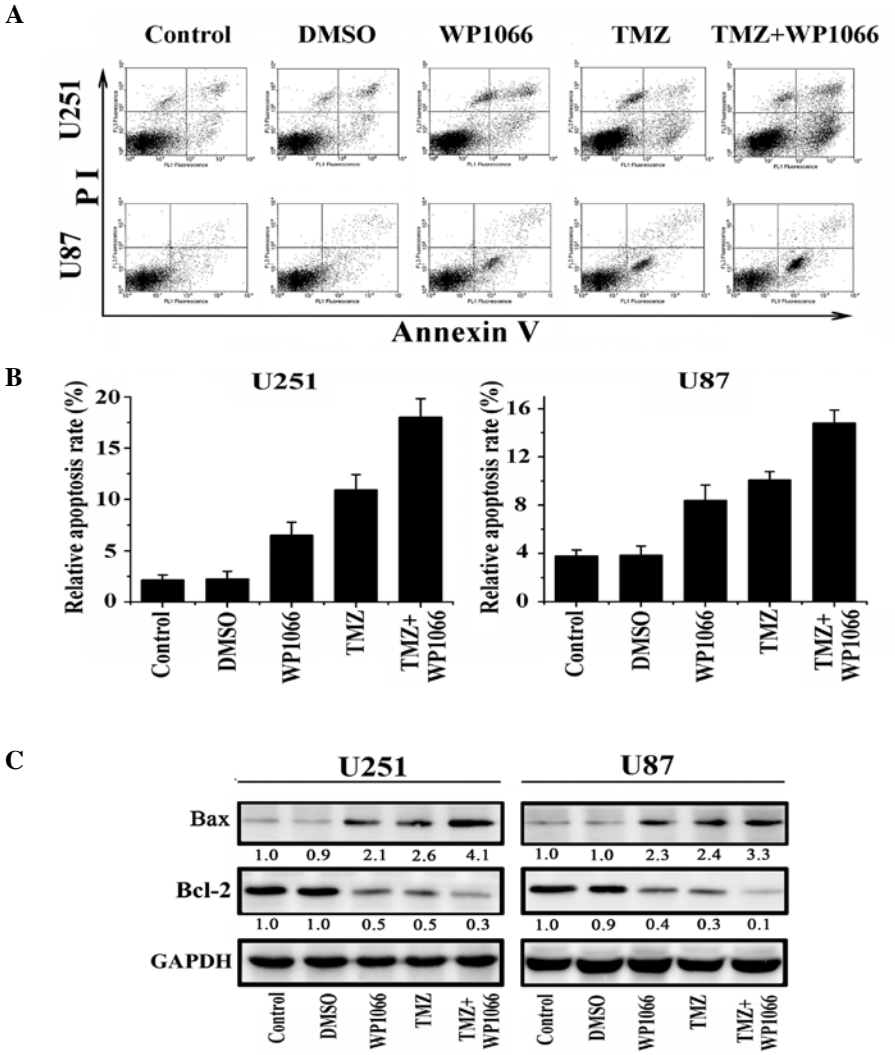


Figure 5. STAT3 inhibition impacts U251 and U87 cell apoptosis. (A) Flow cytometric analyses of propidium iodide (PI)-stained cells, performed in triplicate. (B) Percentage of apoptotic cells is shown in the histograms. (C) Representative Western blots reveal the altered levels of the apoptosis-regulating proteins Bcl-2 and Bax.

tumorigenesis (21). We showed that TMZ (10 $\mu$M)-induced inhibition of β-catenin was regulated by STAT3 activation. While TMZ inhibited β-catenin by 40% in both U251 and U87 cells, a 50% reduction in p-STAT3 by WP1066 enhanced the inhibition of β-catenin to 60% (Fig. 3). Taken together, TMZ-induced inhibition of the p-AKT and β-catenin pathways is regulated by p-STAT3.

*WP1066 enhances TMZ-induced cytotoxicity of U251 and U87 cells*. To determine whether inhibition of STAT3 sensitizes U251 and U87 cells to TMZ-induced cell death, dose-response curves for TMZ were generated alone and in combination with WP1066. The results revealed that WP1066 decreases proliferation and increases U251 and U87 cell sensitivity to TMZ. Fig. 4A shows that the TMZ concentration causing 50% growth inhibition ($IC_{50}$) of U251 cells was reduced from 22 to 6 $\mu$M when administered in combination with 3 $\mu$M WP1066 ($P<0.01$). Similarly, combination treatment with WP1066 reduced the $IC_{50}$ of TMZ in U87 cells from 23 to 5 $\mu$M ($P<0.01$). The combination of WP1066 and TMZ resulted in enhanced efficacy over TMZ alone throughout the 6-day experiment (Fig. 4C and D).

*WP1066 sensitizes glioma cells to TMZ-induced apoptosis and $G_0$-$G_1$ arrest*. FACS analysis was performed to detect DNA fragmentation indicative of apoptosis following combined administration of WP1066 and TMZ in U251 and U87 cells (Fig. 5A). Untreated cells served as a negative control. Compared with TMZ (11.22 and 9.11% in U251 and U87 cells, respectively) or WP1066 (6.38 and 8.19%, respectively) alone, combination of WP1066 and TMZ therapy resulted in a significant increase in apoptotic cell death (18.56 and 14.77% in U251 and U87 cells, respectively; percentage of apoptosis is shown as histograms in Fig. 5B; $P<0.05$). A significant decrease in the expression of Bcl-2, a potent anti-apoptotic regulatory factor, was observed following treatment of U251 and U87 cells with TMZ combined with WP1066, compared to treatment with TMZ alone (Fig. 5C; $P<0.05$). Similarly, the expression of pro-apoptotic Bax was >50% increased in each cell line following treatment with TMZ plus WP1066, compared to TMZ alone (Fig. 5C; $P<0.01$).

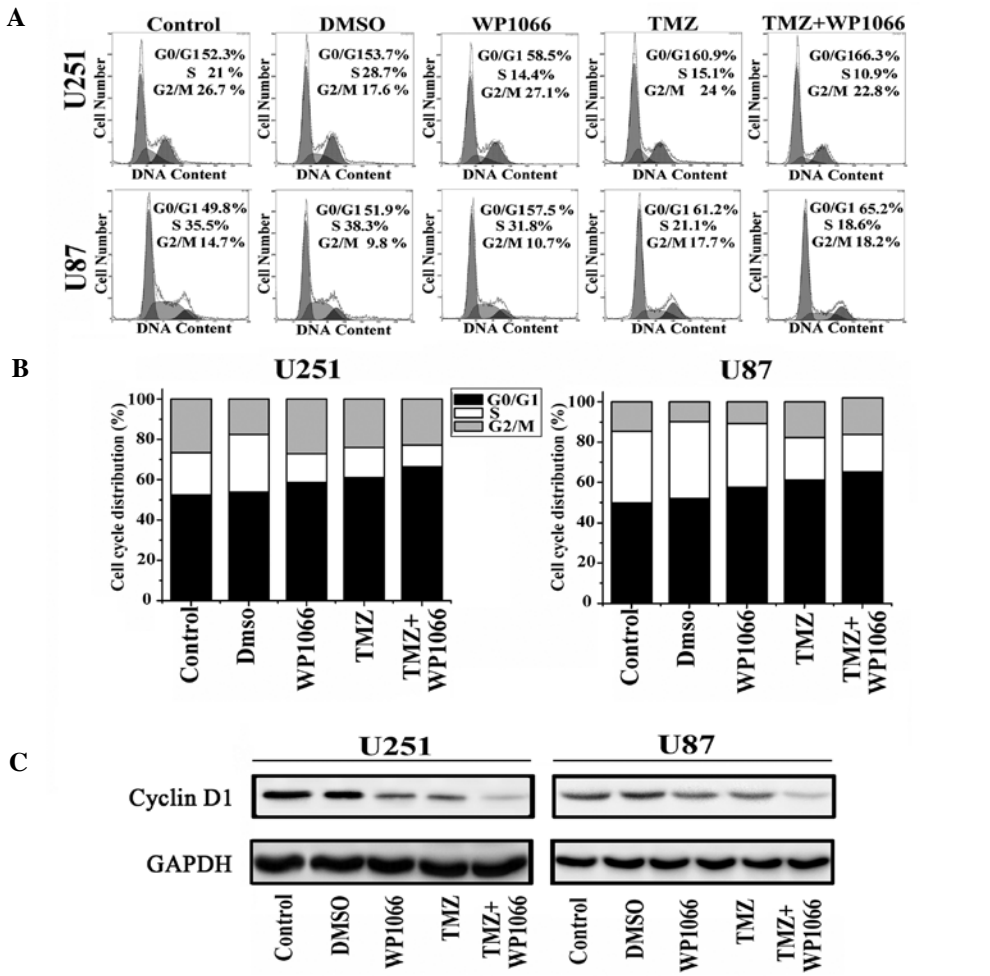


Figure 6. STAT3 inhibition impacts cell cycle distribution. (A and B) U251 and U87 cells were treated with WP1066 and TMZ alone or in combination, and cell cycle distributions were detected by flow cytometry 48 h thereafter. (C) Western blot analysis reveals altered Cyclin D1 activity upon STAT3 inhibition in both U251 and U87 cells.

Collectively, these data suggest that inhibition of STAT3 sensitizes glioblastoma cells to TMZ-induced apoptosis.

To investigate the synergistic effects of WP1066 and TMZ on cell cycle progression, cell cycle phase distribution was determined by flow cytometric analysis. When combined with WP1066, TMZ significantly increased the population of cells at the $G_0$-$G_1$ boundary (Fig. 6A and B; $P<0.01$) and down-regulated the expression of the cell cycle-regulating protein Cyclin D1 (Fig. 6C), compared to treatment with TMZ alone.

## Discussion

A growing body of evidence indicates that constitutively activated STAT3 in malignant glioma is correlated with a poor clinical outcome (5,6,8). However, the role of STAT3 in chemoresistance remains unknown. In this study, we analyzed 68 GBM patients receiving a similar treatment protocol of alkylating agents, using pY705-STAT3 as a measure of STAT3 activation. We found that p-STAT3 was a significant independent unfavorable prognostic factor for GBM progression and prognosis. Furthermore, inhibition of STAT3 increased TMZ-induced cell death in U251 and U87 cells, reducing the drug $IC_{50}$ by 3.7- and 4.6-fold, respectively. FACS analysis showed that a STAT3 inhibitor enhanced TMZ-induced apoptosis and induced $G_0$-$G_1$ arrest. These results indicate that aberrant activation of STAT3 confers alkylator-resistance, suggesting that targeting STAT3 can enhance glioma cell chemosensitivity. Our findings identify a novel approach to improve therapy for GBM.

Accumulating experimental evidence indicates that constitutive activation of the P13K/AKT signaling pathway is associated with tumor cell resistance to conventional chemotherapy (19,20). To our knowledge, this is the first study to investigate whether the blockade of the p-AKT pathway by alkylator treatment is related to p-STAT3 expression. We found that glial tumor cells with hyperactive STAT3 tend to express high levels of p-AKT, and TMZ has only a modest impact on AKT activation in these cells. The effectiveness of TMZ was dramatically enhanced upon inhibition of STAT3. These results suggest that STAT3 confers alkylator-resistance, in part by up-regulating the PI3K/AKT signaling pathways.

β-catenin is a key factor in the Wnt signaling pathway. The elevation of β-catenin levels leads to its nuclear accumulation and forms a β-catenin/Lef/Tcf complex and regulates transcription of multiple genes involved in apoptosis and cell cycle, including c-myc and Cyclin D1 (11). Therefore, aber-

rant activation of the β-catenin pathway also has potential to contribute to alkylator-resistance. We observed that inhibition of STAT3 resulted in down-regulation of the protein expression of β-catenin in malignant glioma cells. In agreement with this finding, Kawada *et al* previously reported that inhibition of STAT3 decreased the nuclear localization and transcriptional activity of β-catenin in colon cancer cells (22). A recent study, using chromatin immunoprecipitation, confirmed two STAT3-binding sites located in the gene promoter region of β-catenin in breast cancer (23), indicating that STAT3 is a transcriptional regulator for β-catenin. These data support our conclusion that p-STAT3 regulates TMZ-induced downregulation of β-catenin expression. Thus, our data indicate that inhibition of STAT3 impacts GBM via at least two distinct pathways, by impacting both AKT and β-catenin signaling.

Collectively, our findings indicate that STAT3 activation in GBM regulates resistance to alkylating agents. Inhibition of STAT3 sensitizes TMZ-induced cell death, at least in part, by blocking the p-AKT and β-catenin pathways. STAT3 signaling regulates several critical signaling pathways, including the PI3K/AKT and Wnt/β-catenin pathways, as well as regulates transcription of other receptor tyrosine kinases. Our findings strongly support the hypothesis that STAT3 inhibition improves the clinical efficacy of alkylating agents for the treatment of GBM. These data warrant additional preclinical evaluation of the therapeutic benefit of STAT3 and alkylating agent combination therapy for drug-resistant glioblastoma.

## Acknowledgements

We thank Yuling Yang for the tissue sample collection and clinical data retrieval. This study was supported by grants from the National Key Project of Science and Technology Supporting Programs of China (no. 2007BAI05B08), National Basic Research Program of China (973 Program) (no. 2011CB707804), China National Natural Scientific Found (30971136), Program for New Century Excellent Talents in University (NCET-07-0615), and the Natural Science Foundation of Tianjin Municipal Science and Technology Commission (10SYSYJC28800, 09JZCD17600).

## References

1. Stupp R, Mason WP, van den Bent MJ, *et al*: Radiotherapy plus concomitant and adjuvant temozolomide for glioblastoma. N Engl J Med 352: 987-996, 2005.
2. Sarkaria JN, Kitange GJ, James CD, *et al*: Mechanisms of chemoresistance to alkylating agents in malignant glioma. Clin Cancer Res 14: 2900-2908, 2008.
3. De la Iglesia N, Puram SV and Bonni A: STAT3 regulation of glioblastoma pathogenesis. Curr Mol Med 9: 580-590, 2009.
4. Schlessinger K and Levy DE: Malignant transformation but not normal cell growth depends on signal transducer and activator of transcription 3. Cancer Res 65: 5828-5834, 2005.
5. Birner P, Toumangelova-Uzeir K, Natchev S and Guentchev M: STAT3 tyrosine phosphorylation influences survival in glioblastoma. J Neurooncol 100: 339-343, 2010.
6. Abou-Ghazal M, Yang DS, Qiao W, *et al*: The incidence, correlation with tumor-infiltrating inflammation, and prognosis of phosphorylated STAT3 expression in human gliomas. Clin Cancer Res 14: 8228-8235, 2008.
7. Lee E, Ko K, Joe YA, Kang S and Hong Y: Inhibition of STAT3 reverses drug resistance acquired in temozolomide-resistant human glioma cells. Oncol Lett 2: 115-121, 2011.
8. Lo HW, Cao X, Zhu H and Ali-Osman F: Constitutively activated STAT3 frequently coexpresses with epidermal growth factor receptor in high-grade gliomas and targeting STAT3 sensitizes them to Iressa and alkylators. Clin Cancer Res 14: 6042-6054, 2008.
9. Shah MA and Schwartz GK: Cell cycle-mediated drug resistance: an emerging concept in cancer therapy. Clin Cancer Res 7: 2168-2181, 2001.
10. Yue X, Lan F, Yang W, *et al*: Interruption of beta-catenin suppresses the EGFR pathway by blocking multiple oncogenic targets in human glioma cells. Brain Res 1366: 27-37, 2010.
11. Tetsu O and McCormick F: Beta-catenin regulates expression of cyclin D1 in colon carcinoma cells. Nature 398: 422-426, 1999.
12. Zhang J, Han L, Zhang A, *et al*: AKT2 expression is associated with glioma malignant progression and required for cell survival and invasion. Oncol Rep 24: 65-72, 2010.
13. Testa JR and Bellacosa A: AKT plays a central role in tumorigenesis. Proc Natl Acad Sci USA 98: 10983-10985, 2001.
14. Iwamaru A, Szymanski S, Iwado E, *et al*: A novel inhibitor of the STAT3 pathway induces apoptosis in malignant glioma cells both in vitro and in vivo. Oncogene 26: 2435-2444, 2007.
15. Louis DN, Ohgaki H, Wiestler OD and Cavenee WK (eds): WHO Classification of Tumours of the Central Nervous System. 4th edition. IARC Press, Lyon, 2007.
16. Kononen J, Bubendorf L, Kallioniemi A, *et al*: Tissue microarrays for high-throughput molecular profiling of tumor specimens. Nat Med 4: 844-847, 1998.
17. Ren Y, Zhou X, Mei M, *et al*: MicroRNA-21 inhibitor sensitizes human glioblastoma cells U251 (PTEN-mutant) and LN229 (PTEN-wild-type) to taxol. BMC Cancer 10: 27, 2010.
18. Yoshino A, Ogino A, Yachi K, *et al*: Gene expression profiling predicts response to temozolomide in malignant gliomas. Int J Oncol 36: 1367-1377, 2010.
19. West KA, Castillo SS and Dennis PA: Activation of the PI3K/Akt pathway and chemotherapeutic resistance. Drug Resist Updat 5: 234-248, 2002.
20. Bellacosa A, Kumar CC, Di Cristofano A and Testa JR: Activation of AKT kinases in cancer: implications for therapeutic targeting. Adv Cancer Res 94: 29-86, 2005.
21. Huang K, Zhang JX, Han L, *et al*: MicroRNA roles in beta-catenin pathway. Mol Cancer 9: 252, 2010.
22. Kawada M, Seno H, Uenoyama Y, *et al*: Signal transducers and activators of transcription 3 activation is involved in nuclear accumulation of beta-catenin in colorectal cancer. Cancer Res 66: 2913-2917, 2006.
23. Armanious H, Gelebart P, Mackey J, Ma Y and Lai R: STAT3 up-regulates the protein expression and transcriptional activity of beta-catenin in breast cancer. Int J Clin Exp Pathol 3: 654-664, 2010.